A comprehensive analysis about thermal conductivity of multi-layer graphene with N-doping, -CH_3 group, and single vacancy

Chao Si,[1,2,3] Liang Li,[1,2,3] Gui Lu,[1,2,3] Bing-Yang Cao,[4,a)] Xiao-Dong Wang,[1,2,3,a)] Zhen Fan,[5] and Zhi-Hai Feng[5]

[1]*State Key Laboratory of Alternate Electrical Power System with Renewable Energy Sources, North China Electric Power University, Beijing 102206, China*
[2]*Research Center of Engineering Thermophysics, North China Electric Power University, Beijing 102206, China*
[3]*Key Laboratory of Condition Monitoring and Control for Power Plant Equipment of Ministry of Education, North China Electric Power University, Beijing 102206, China*
[4]*Key Laboratory for Thermal Science and Power Engineering of Ministry of Education, Department of engineering mechanics, Tsinghua University, Beijing 100084, China*
[5]*Key Laboratory of Advanced Functional Composite Materials, Aerospace Research Institute of Materials and Processing Technology, Beijing 100076, China*

(Received 23 October 2017; accepted 17 March 2018; published online 2 April 2018)

Graphene has received great attention due to its fascinating thermal properties. The inevitable defects in graphene, such as single vacancy, doping, and functional group, greatly affect the thermal conductivity. The sole effect of these defects on the thermal conductivity has been widely studied, while the mechanisms of the coupling effects are still open. We studied the combined effect of defects with N-doping, the -CH_3 group, and single vacancy on the thermal conductivity of multi-layer graphene at various temperatures using equilibrium molecular dynamics with the Green-Kubo theory. The Taguchi orthogonal algorithm is used to evaluate the sensitivity of N-doping, the -CH_3 group, and single vacancy. Sole factor analysis shows that the effect of single vacancy on thermal conductivity is always the strongest at 300 K, 700 K, and 1500 K. However, for the graphene with three defects, the single vacancy defect only plays a significant role in the thermal conductivity modification at 300 K and 700 K, while the -CH_3 group dominates the thermal conductivity reduction at 1500 K. The phonon dispersion is calculated using a spectral energy density approach to explain such a temperature dependence. The combined effect of the three defects further decreases the thermal conductivity compared to any sole defect at both 300 K and 700 K. The weaker single vacancy effect is due to the stronger Umklapp scattering at 1500 K, at which the combined effect seriously covers almost all the energy gaps in the phonon dispersion relation, significantly reducing the phonon lifetimes. Therefore, the temperature dependence only appears on the multi-layer graphene with combined defects. *Published by AIP Publishing.*
https://doi.org/10.1063/1.5010091

I. INTRODUCTION

Graphite nanosheets are the important matrix materials in thermal conductive composites, which have the multi-layer graphene (MLG) structure with 2–30 layers and in-plane sizes of 1–100 μm.[1] They are one of the high thermal conductivity materials which can be used in the shell of spacecrafts,[1] the nose and wings of missiles,[2] and the aft end of rockets,[3] and they always work at extremely high temperature conditions.[3]

High thermal conductivity can only be obtained for the perfect MLG with ideal structures. However, in practical applications, there inevitably exist atomistic alterations or defects within the honeycomb lattice of MLG, including vacancy,[4] doping,[5] functional group,[6] grain boundary,[7] edge roughness,[8] and so on. The ideal MLG can be regarded as the AB-stacking of single-layer graphene (SLG). It is commonly known that defects can significantly reduce the thermal conductivity of graphene since the phonon transport in SLG can be strongly affected by the different types of defects. Pop *et al.*[9] have summarized the influences of the different defects, such as vacancy, doping, and functional group, on thermal conductivities of SLG.

The effects of vacancy,[10–15] doping,[16–18] or the functional group[19] on thermal conductivity of SLG have been widely studied. Hao *et al.*[4] and Haskins[10] studied the in-plane heat transfer processes in the SLG investigated in the real space. The single defect was equivalently treated as a thermal resistance within the graphene sheet to obtain the temperature field. Such early work cannot provide phonon transport details, which strongly affect the thermal properties of SLG. Therefore, the phonon density of states (DOS) of the defected SLG was used later[11–13] to roughly characterize the defect scattering of the phonon. Recently, Feng *et al.*[14] introduced the method of the normal mode analysis (NMA) to obtain the accurate parameters of phonon branches in the defected SLG, which can reveal the effects of the defects on group velocities and lifetimes of all the phonon branches.

[a)]Authors to whom correspondence should be addressed: caoby@tsinghua.edu.cn, Tel./Fax: +86-10-62794531 and wangxd99@gmail.com, Tel./Fax: +86-10-62321277.

Most previous work focused on the effect of sole defects on the thermal properties of the graphene sheet. In practical, there are several types of defects in the graphite nanosheet. Few works[20–22] have studied the combined effects of various types of defects on the thermal properties. Islam *et al.*[22] revealed the combined effects of doping and vacancy defects on phonon DOS using forced vibrational method. Yang's group[20,21] found that different shapes of N doping near a vacancy hole in SLG can significantly change the DOS curve. Their work shows that when all the types of defects co-exist within one MLG, the coupling effects should be considered. Such a conjecture is supported by the experiments of Balandin's group.[23] They observed that the thermal conductivities of MLG decrease with the increasing amount of defects, but the decreasing rate is different from that predicted by the simulation of SLG with single vacancy, which implies that there should be coupling effect between the functional group defects and the vacancy defects. However, the mechanism of coupling effects is still unclear. In addition, how to evaluate the coupling effect of various types of defects is a key issue to tune the thermal properties of MLG.

In this work, the sole effect and coupling effects of vacancy, doping, and functional group defects on thermal conductivities and phonon properties using molecular dynamics simulations are studied. The Taguchi orthogonal algorithm[24] is used to evaluate the coupling effects with limited simulations. The amounts of defects are chosen based on the experimental results. The normal mode analysis is used to obtain the accurate parameters of phonon branches, which can provide microscopic understanding for the thermal properties modification of MLG caused by various defects. The aim of this work provides not only a simple but effective way to evaluate the coupling effect of various defects on the thermal properties of MLG but also a guideline to tune the thermal conductivity graphene materials.

II. SIMULATION METHODS

A. Molecular dynamics simulation

The traditional equilibrium molecular dynamics (EMD) simulation method[25] is utilized to study the effects of defects on thermal conductivities of multi-layer graphene. First, the studied MLG without any defects is built in the Large-scale Atomic Molecular Massively Parallel Simulator (LAMMPS) packages,[26] as shown in Fig. 1(a). The origin size of one graphene sheet in the MLG is 87.0×74.8 Å^2, which contains 2400 atoms. The MLG has 10 layers, and the thickness is 34.0 Å. The chirality of the MLG in the x-direction in Fig. 1(a) is armchair. The periodic boundary conditions are fixed in the x- and y-directions, and the free boundary condition is fixed in the z-direction. The MLG with defects including the vacancies, the doping, and the functional group can be achieved by randomly adding theses defects into the MLG. The types of defects are determined based on the experimental observation. For the vacancy defect, Ref. 10 has revealed that among all the vacancy types, such as the single vacancy, the double vacancy, and the Stone-Wales vacancy, the single vacancy greatly affects the thermal conductivity. Thus, in this work, the single vacancy is chosen, which is created by randomly deleted the non-adjacent C atoms in the sheets of MLG based on the certain vacancy percentage, as shown in Fig. 1(b). The nitrogen atom is chosen due to its important applications in electrochemical and electrothermal reactions.[16–18] Besides, the atom type can only cause a slight quantitative difference of phonon scattering in MD simulation. How the doping scatters the phonon is independent of atom types. Hence, nitrogen atoms are chosen as the doping atoms, which randomly replace the C atoms in the sheets, as shown in Fig. 1(c). For the functional group defect, it has been qualitatively proven that the phonon scattering caused by the functional group is related to the mass and the angular momentum of the defect functional group.[19] As a comparison study, the common -CH_3 groups are chosen as the functional group defects.

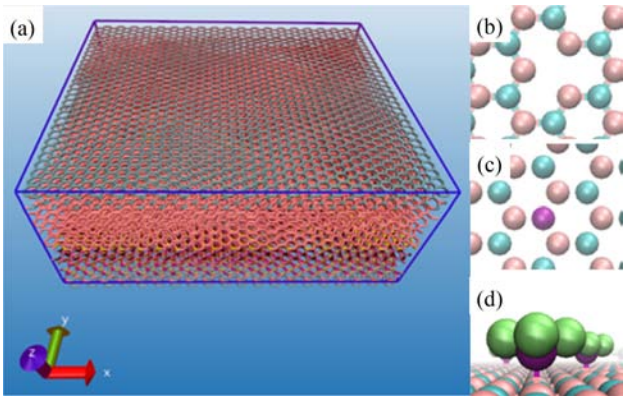

FIG. 1. Schematic diagrams of (a) the10-layer graphene with the sheet size of 87.0×74.8 Å^2, (b) the single vacancy, (c) N-doping, and (d) -CH_3 group.

In the EMD approach, the opt-Tersoff potential model[27] is utilized to describe the intralayer interactions between C atoms in one sheet. The 12-6 Lennard-Jones (LJ) is used to model the interlayer interactions, which can be expressed as

$$V_{ij}^{\mathrm{LJ}} = 4\varepsilon_{ij}\left[\left(\frac{\sigma_{ij}}{r_{ij}}\right)^{12} - \left(\frac{\sigma_{ij}}{r_{ij}}\right)^{6}\right], \tag{1}$$

where V_{ij}^{LJ} is the potential between atoms i and j, r_{ij} denotes the atomic distance between i and j, and ε_{ij} and σ_{ij} are the minimum energy and the zero energy separation distance, respectively. For C atom pairs, $\sigma_{ij} = 3.4$ Å and $\varepsilon_{ij} = 0.00251$ eV. Since there may be doped N atoms in the graphene sheets, the C-N intralayer interactions are defined via the C-N Tersoff parameters.[28] The interaction modified parameters for the C-N bonding are set as $\chi_{ij} = 0.9685$ and $\omega_{ij} = 0.6381$.[28] Interlayer interactions between C and N atoms are based on the mixture rule, as shown in Table I. The bond lengths between two sp^3 C atoms are set as 1.54 Å, while all the bond lengths between two sp^2 C atoms are 1.44 Å. The mixture rule also works for the bond lengths of

TABLE I. The mixture rule of interlayer LJ parameters.

Atoms	σ (Å)	ε (eV)
C	3.4	0.00251
N	3.71	0.00725
The mixture of C and N LJ interactions	3.555	0.00427

sp^2-sp^3 C-C bonding. Due to the lacking of a proper method for simulating the sp^2-sp^3 C-C interactions which should also guarantee the accuracy of the thermal conductivity, all the C-C interactions in graphene with the -CH_3 group and N-doping are described by the opt-Tersoff potential. For the -CH_3 group added on the graphene sheets, the traditional AIREBO[29] potential model is utilized to describe the C-H bonding characteristics.

The EMD simulations are carried to obtain the polarized information of each atom. The time step of the simulations is set as 0.001 ps. The defect MLG is located in the simulation box whose size keeps $87.0 \times 74.8 \times 500$ Å^3. The boundary conditions are periodic along x- and y-directions and free in the z-direction. To establish the MLG in the equilibrium state, two stages are run in the MD simulation. First, the isothermal-isobaric ensemble (NPT) control of 300 ps is carried out at temperatures of $T_{MD} = 300$ K, 700 K, and 1500 K and a pressure of 0 Pa. Then, the following microcanonical ensemble (NVE) control of 600 ps is performed. The time evolution of the system energy is tested to ensure that the equilibrium state can be kept. The thermal conductivity of the defect MLG can be calculated by Green-Kubo theory[25] in the later NVE control of 2 ns. The Green-Kubo theory can be expressed as

$$\lambda_x = \frac{V}{k_B T^2} \int_0^\infty \langle J_x(0) J_x(t) \rangle \mathrm{d}t, \tag{2}$$

where λ_x denotes the thermal conductivity in the x-direction, V is the volume of the MLG, k_B is the Boltzmann constant, T is the temperature, $J_x(t)$ is the heat flux in the x-direction J_x at time t, and $\langle\rangle$ denotes the ensemble average. Considering that the opt-Tersoff and C-N Tersoff are many-body potential models, the heat flux $J_x(t)$ is calculated by the theory raised by Li *et al.* as follows:[30]

$$\mathbf{J} = \frac{1}{V}\left(\sum_{i=1}^{n} \vec{v}_i \varepsilon_i + \frac{1}{2}\vec{r}_{ij}\left(\Delta\vec{F}_j \cdot \vec{v}_j - \Delta\vec{F}_i \cdot \vec{v}_i\right) - \frac{1}{2}\left(\vec{r}_{jk} - \vec{r}_{ki}\right)\left(\Delta\vec{F}_k \cdot \vec{v}_k\right)\right), \tag{3}$$

where $\mathbf{J} = (J_x, J_y, J_z)$ is the heat flux vector, $\vec{v}_i$ is the velocity vector of atom i, ε_i is the internal energy of atom i, $\vec{r}_{ij} = \vec{r}_i - \vec{r}_j$ is the distance vector from atom i to atom j, $\Delta\vec{F}_i$ is the contribution of atom i to the many-body potential $W_{ijk}^{\mathrm{Tersoff}}$ among the atoms i, j, and k, and $\Delta\vec{F}_\alpha = -\partial W_{ijk}^{\mathrm{Tersoff}}/\partial\vec{r}_\alpha$ for $\alpha = i, j$, and k. Since all the defects are randomly added to the graphene sheets in MLG, the thermal conductivity of each defected MLG with a certain addition ratio is predicted by averaging the results of 10 repetitive simulations. For the EMD simulations at $T_{MD} = 300$ K, there exist considerable error introduced by the quantum effect, so that the quantum correction is needed when predicting the thermal conductivity using Eq. (2). Based on the empirical correlation in Ref. 31, the correction coefficient of $\mathrm{d}T_{MD}/\mathrm{d}T = 0.851$ is adopted. For $T_{MD} = 700$ K and 1500 K, the quantum effect can be neglected.[31]

To reveal the phonon characteristics in the defected MLG, the spectral energy density (SED) method developed by McGaughey's group[32] is employed to calculate the phonon dispersion relation in the NMA approach. Similar to Ref. 14, it is assumed that all the defects within the MLG can hardly affect the lattice symmetry. In the SED method, the spectral energy density of the phonon with wave vector $\mathbf{q}_\beta$ at frequency ω in the β-direction, Φ, can be analytically expressed as

$$\Phi(\mathbf{q}_\beta, \omega) = \frac{1}{4\pi\tau_0 l}\sum_{\alpha,b} m_b \left\| \int_0^{\tau_0} \sum_l \dot{u}_\alpha(l,b) \exp\left(\mathrm{i}\mathbf{q}_\beta \cdot \mathbf{r}(l,0) - \mathrm{i}\omega t\right)\mathrm{d}t \right\|^2, \tag{4}$$

where m_b is the mass of the b atom in the l unit cell, $\dot{u}_\alpha(l,b)$ is the velocity of this atom in the α-direction, τ_0 is the calculation time range which is equal to the time range of calculating the phonon normal coordinate in the MD simulation and $\tau_0 = 2$ ns in this work, $\mathbf{r}(l, 0)$ is the balance distance vector of the lth unit cell, and i is the imaginary unit. Since the MLG studied in this work is a three-dimensional structure, the spectral energy density Φ can be divided into 6 branches to obtain the phonon characteristics in three directions.

B. Taguchi orthogonal algorithm

As shown in Table II, 192 simulations are needed if we want to study the effects of three defects, with 4 loadings for each, at three different temperatures. To find the rational coupling effects when so many factors involved with limited simulations, the Taguchi orthogonal algorithm[24] is introduced to simplify the analysis process. The Taguchi method can classify the experimental results by employing an orthogonal array, consisting of factors and levels. This algorithm has been used to seek the best results of experimental results and simulations.[33] Meanwhile, the sensitive of the factors on the physical behavior can be obtained by introducing the signal-to-noise (S/N) ratio, where the signal denotes the desired real value and noise denotes the undesired factors. A larger S/N ratio corresponds to a better performance or quality of a system. Also, the S/N ratio has always been used to stand for the engineering quality in the analysis of the Taguchi method.

In this work, the basic categories of the thermal conductivity of MLG in the Taguchi approach should be the larger-the-better because the larger thermal conductivity is needed for the material in practice. The S/N ratio in terms of thermal conductivity can be expressed as

$$S/N(y) = -10\log_{10}\left(\frac{1}{n}\sum\frac{1}{y^2}\right), \tag{5}$$

TABLE II. Factors, control parameters, and levels.

Factor	Control parameter	Level 1	2	3	4
A	Amount ratio of doping N atoms	1%	2%	3%	4%
B	Amount ratio of functional group	2%	4%	6%	8%
C	Amount ratio of single vacancy	1%	2%	3%	4%

TABLE III. Level combination of different amount ratios of the defects in the $L_{16}(4^3)$ orthogonal array.

	Factor		
Case	A	B	C
1	1	1	1
2	1	2	2
3	1	3	3
4	1	4	4
5	2	1	2
6	2	2	1
7	2	3	4
8	2	4	3
9	3	1	3
10	3	2	4
11	3	3	1
12	3	4	2
13	4	1	4
14	4	2	3
15	4	3	2
16	4	4	1

where y represents the values of thermal conductivities and n is the time of the repetitive tests. Since the thermal conductivity of each defected MLG with certain factors is predicted by averaging the results of 10 repetitive simulations, $n = 10$.

The three types of defects are treated as the control parameters in the Taguchi approach. Each parameter with four levels is taken into account. The amount ratio of vacancy ranges from 1% to 4% since the structural failure occurs less if the amount of vacancy is larger than 4%.[34] The loadings of the N-doping defect range from 1% to 4% in the simulations since the N-doping loadings slightly affect the thermal conductivity if they are larger than 5%, even though the 8% N-doping has been reported.[17,34] The range of the functional group defect amount ratio is chosen as 2%–8% according to Ref. 19. Correspondingly, a typical orthogonal array $L_{16}(4^3)$ with 16 runs is designed in Table III. Owing to the Taguchi orthogonal algorithm, the coupling effects of three types of defects can be evaluated with only 48, not 196 runs, without losing any of generality. Thus, the weight analysis for the effects of different types of defects on the thermal conductivity of MLG can be implemented.

III. RESULTS AND DISCUSSION

The three factors of defect types and four amount levels are considered in the EMD simulation to study their effects on the thermal conductivity of 10-layer graphene with the sheet size of 87.0×74.8 Å^2. Although the sole effects of defects on thermal conductivity of SLG have been widely studied, the sole factor analysis is still needed when we study the effects of defects on the thermal conductivity of MLG, which can be regarded as the baseline when we study their combined effects.

A. Sole factor analysis

EMD simulation is employed to calculate the thermal conductivities of MLG with the sole type of defect including 1%–4% N-doping, 2%–8% -CH_3 group, or 1%–4% single vacancy, as shown in Fig. 2. For the three defects, the thermal conductivity decreases with increasing defect loadings. The thermal conductivity curves of 300 K and 700 K almost overlap with each other for the three defects but diverge from that of 1500 K. For example, the thermal conductivities of the MLG with 4% N-doping are 759.1 W m^{-1}K^{-1} at 300 K and 817.2 W m^{-1}K^{-1} at 700 K but 211.9 W m^{-1}K^{-1} at 1500 K. Based on Ref. 35, with the increasing temperature from 300 K to 1500 K, the thermal conductivity should increase first and decrease later, and the peak is near 400 K. The temperature effect is caused by the competition between the temperature dependence of specific heat and the Umklapp scattering. The lattice thermal conductivity is proportional to the specific heat, while the Umklapp scattering can introduce the thermal resistance to the graphene and is disadvantageous for the heat conduction. For $T_{MD} < 700$ K, specific heat is positively correlated with the temperature, while the effect of Umklapp scattering is not strong enough to cover the effect of the specific heat. Hence, the thermal conductivities of MLG containing defects at 300 K and 700 K are similar. For $T_{MD} > 700$ K, the Umklapp scattering becomes very strong because there are more exited phonons near the boundary of the wave-vector space. Hence, the thermal conductivities drop significantly at 1500 K.

Moreover, since of the defects always reduce the thermal conductivities of MLG due to the additional thermal resistance caused by extra phonon impurity scattering, the

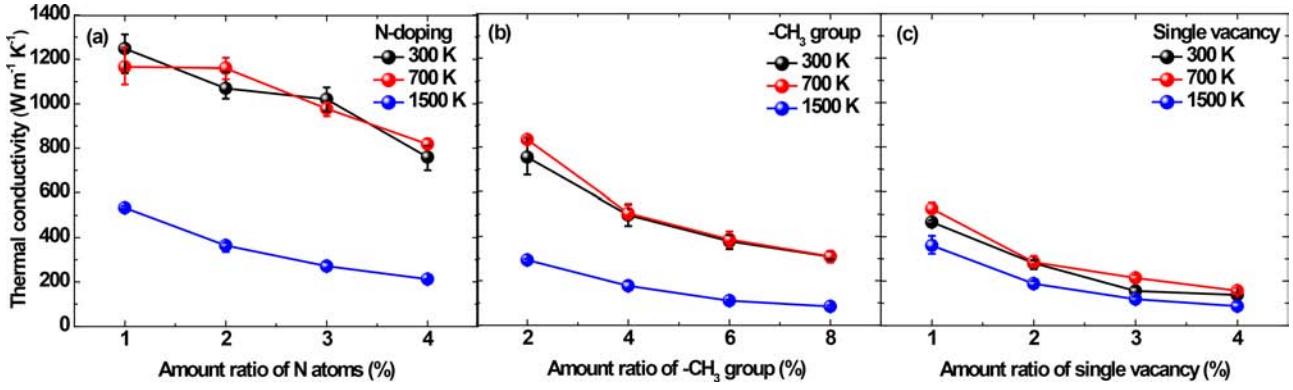

FIG. 2. The thermal conductivities of the MLG with the single type of defect, including (a) 1%–4% N atoms, (b) 2%–8% -CH_3 group, and (c) 1%–4% single vacancy at 300 K, 700 K, and 1500 K.

importance degree of each defect type can be characterized by the declines of the thermal conductivities. Stronger phonon impurity scattering will lead to a lower thermal conductivity at the same temperature. At 300 K and 700 K, the single vacancy significantly reduces the thermal conductivity, while the N-doping has the fewest effects on the thermal conductivity. For example, the thermal conductivity for MLG with 2% single vacancy is only 300 W $m^{-1}K^{-1}$ at 300 K but 1100 W $m^{-1}K^{-1}$ for the MLG with 2% N-doping at the same temperature, so does the temperature of 1500 K, as shown in Fig. 3. The simulation results are compared with the recent literature,[23] as shown in Fig. 4. A similar decreasing trend can be found in both the simulation and the experiment. The thermal conductivity of graphene with defects decreases faster at lower defect density, while it decreases slower at higher defect density. The absolute values of MD simulation are lower than those of the experiment due to the domain-size limitation in the simulation, which has been indicated by Ref. 23, since the graphene size in the experiment is on the macroscale.

To quantify the effects of the defects on phonon impurity scattering, the NMA analysis will be carried out. Figure 5 shows the phonon dispersion relation of MLG with various types of defects at 300 K. Compared with the perfect MLG, both the N-doping and the -CH_3 group can widen the energy band of branches. From the physical point of view, a wider energy band indicates a shorter phonon lifetime for each branch since the positions of branches are kept fixed. The widening for the 1% N-doping mainly occurs on the TO and LO branches. Such widening becomes more significant for the MLG with 4% N-doping and the 2% -CH_3 group. For MLG with the 4% -CH_3 group and 1% vacancy defects, the widening occurs on every branch at every wavevector length. For the MLG with 4% vacancy defects, the widening becomes more obvious. Moreover, some unexpected bands can be found in the vacancy cases. In the previous studies, Haskins *et al.*[10] reported that the single vacancy in SLG is a kind of defect with high energy, which can create the two-coordinate bond for three C atoms. The above conclusion is obtained by the analysis in the real space, while Fig. 5

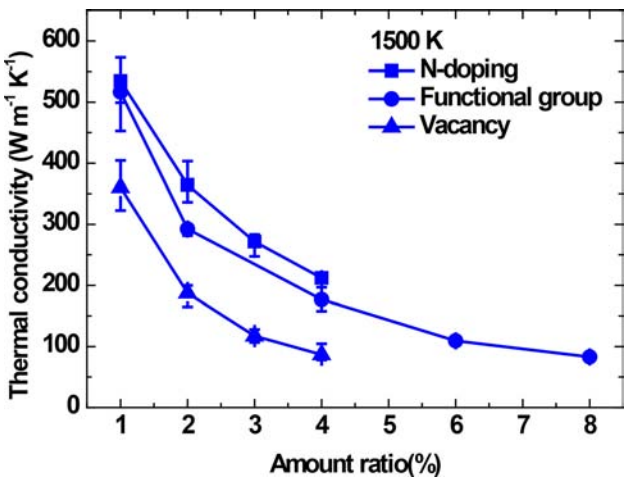

FIG. 3. The thermal conductivities of MLG with the three respective types of defects at 1500 K.

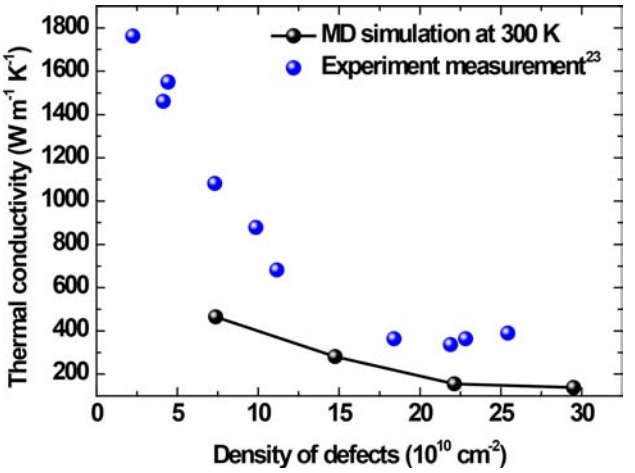

FIG. 4. The comparison of the thermal conductivities between the MD simulation and the experimental measurement.[23]

reflects that the high energy of single vacancy excites the extra phonon at a high energy level. The extra phonon can be attributed to the phonon localization phenomenon near the vacancy.[4,14,37] Hao *et al.*[4] and Loh *et al.*[37] have pointed out that the phonon localization phenomenon near a single vacancy in SLG is inevitable, and the frequency of the localization phonon, which denotes the extra phonon excited by the localization phenomenon, is larger than 50 THz.[14] They also attributed the inhibition of the heat transfer to the strong interaction between the localization phonon and the low-frequency phonon. According to the horizontal dispersion curve of the localization phonon as shown in Fig. 5, the group velocities of the extra phonon are almost zero, which can be regarded as the direct evidence of localization. The near-zero group velocities also lead to the deterioration heat transfer in MLG with vacancy.

Figure 6(a) shows the semi-logarithmic plot of the SED at the M point in the first Brillouin zone for MLG with 4% N-doping, 4% -CH_3 group, and 4% vacancy, which can quantitatively compare the phonon lifetimes for the different types of defects. The larger half width of each peak indicates the smaller phonon lifetime according to the NMA approach. It can be found that the peaks in the curve of 4% vacancy are much wider. In addition, the extra exited phonon in MLG with 4% vacancy leads to two extra peaks at the frequencies of 57.8 THz and 66.2 THz.

Based on the lattice dynamics, Fig. 6(b) shows the phonon lifetimes at the M point in the first Brillouin zone, which are calculated. MLG with 4% N-doping has the longest phone lifetimes for almost all the phonon branches. For the flexural acoustic (ZA) branches, the phonon lifetime of 4% N-doping MLG is 0.58 ps, while the 4% -CH_3 group is 0.20 ps and 4% vacancy MLG is 0.14 ps. The phonon impurity scattering for the N-doping is weak. As shown in Fig. 6(b), the phonon impurity scattering for the -CH_3 group is stronger for ZA, LA, LO, and TO branches, where L denotes longitudinal, T denotes transverse, O denotes optical, and A denotes acoustic. Phonon lifetimes of 4% vacancy MLG are the shortest for all the branches. According to the half width of each peak in Fig. 6(a), the vacancy defect might strongly affect the lattice

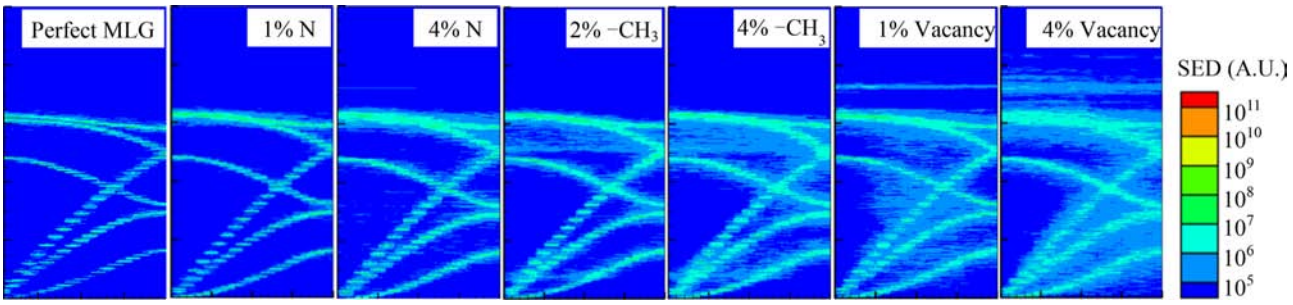

FIG. 5. The phonon dispersion relation of MLG with each single type of the defect at 300 K.

dynamics properties and hence destroy the lattice symmetry. Therefore, the phonon impurity scattering of the vacancy defect is the strongest. The extra high frequency phonon excited by the vacancy defect further inhibits the phonon transport in the MLG, leading to the smallest thermal conductivities of MLG with vacancy at 300 K, 700 K, and 1500 K.

B. Multi-factor analysis

When all the types of defects are added to the MLG, the Taguchi orthogonal algorithm is utilized to analyze the combined effects of 1%–4% N-doping, 2%–8% -CH_3 group, and 1%–4% single vacancy on the thermal conductivities of MLG at 300 K, 700 K, and 1500 K. According to the level combination of different amount ratios of the defects listed in Table III, the thermal conductivities of 16 cases are calculated using the EMD method, as shown in Fig. 7. Also, the temperature effect can be easily found, which can be explained by the competition of the temperature effects of specific heat and the phonon Umklapp scattering. Among the 16 cases, the maximum thermal conductivity of 327.5 W $m^{-1} K^{-1}$ is exhibited at case #1 (with 1% N-doping, 2% -CH_3, and 1% single vacancy) at 300 K, whereas the minimum thermal conductivity of 80.7 W $m^{-1} K^{-1}$ occurs at case #4 at 300 K. The pronounced difference between these two cases reveals that the combination of the 3 factors should play an important role in the heat transfer in defected MLG.

The mean S/N ratio of each factor can be obtained based on the thermal conductivities calculated by 16 cases. For example, the mean S/N ratio of Factor A at Level 1 in terms of thermal conductivity is equal to $[S/N(\lambda_1) + S/N(\lambda_2) + S/N(\lambda_3) + S/N(\lambda_4)]/4$, where λ_1, λ_2, λ_3, and λ_4 are the mean thermal conductivities of case 1, case 2, case 3, and case 4. These 4 cases are chosen to calculate the mean S/N ratio of Factor A at level 1 because they contain all the level 1 values for Factor A. The other mean S/N ratios are calculated by the same procedure. The profiles of the mean S/N ratio of the 3 factors at 300 K, 700 K, and 1500 K are plotted in Fig. 8. The effect of each factor can be calculated by the difference

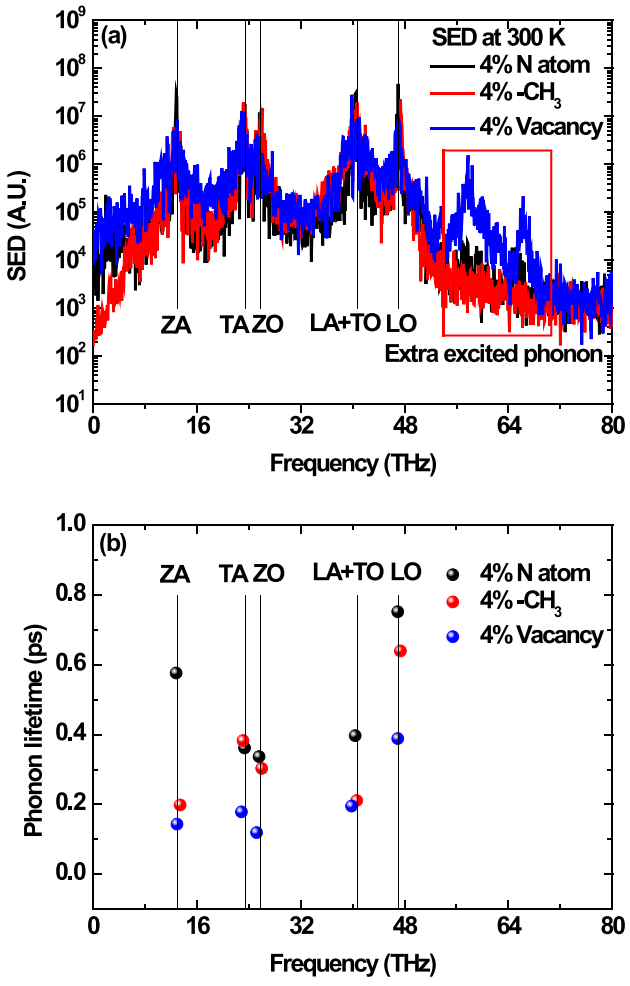

FIG. 6. (a) The semi-logarithmic plot of the SED at the M point in the first Brillouin zone for MLG with 4% N-doping, 4% -CH_3 group, and 4% vacancy and (b) the phonon lifetimes of the MLG at the M point in the first Brillouin zone.

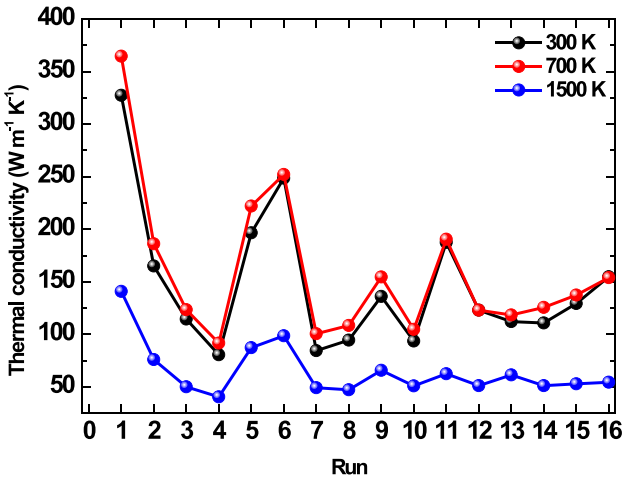

FIG. 7. Thermal conductivities of MLG with defects listed in the $L_{16}(4^3)$ orthogonal array at 300 K, 700 K, and 1500 K.

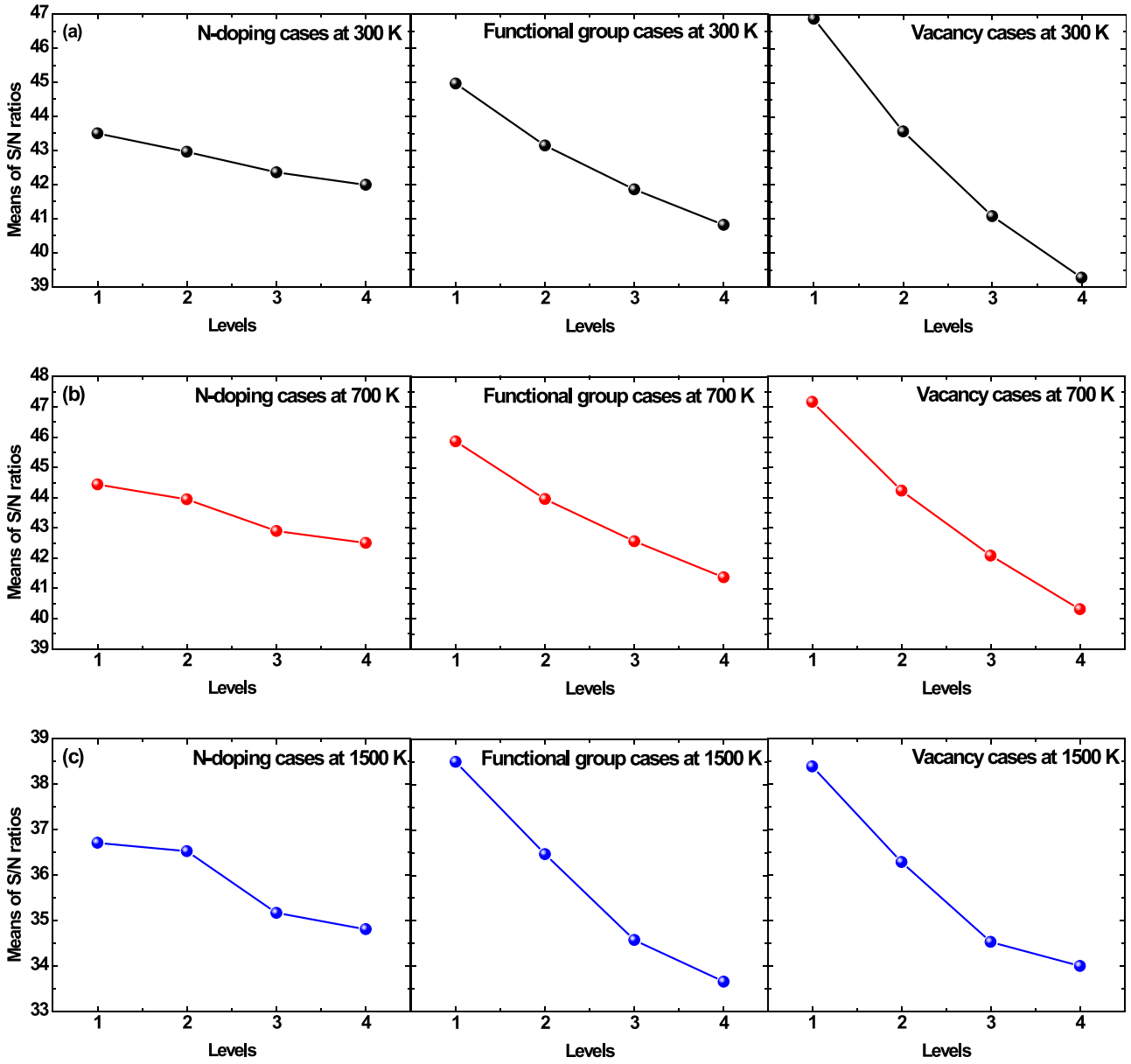

FIG. 8. The mean S/N ratios of the thermal conductivities of MLG with defects listed in the $L_{16}(4^3)$ orthogonal array at (a) 300 K, (b) 700 K, and (c) 1500 K.

between the maximum mean S/N ratio and the minimum one. A larger mean S/N ratio corresponds to a stronger impact of the factor on the thermal conductivity. As shown in Fig. 8, the effect of the N-doping factor on thermal conductivity is the weakest among the 3 factors at 300 K, 700 K, and 1500 K, which have the smallest differences between the maximum and the minimum mean S/N ratios. The single vacancy factor plays the most important role on the thermal conductivity at 300 K and 700 K according to Figs. 8(a) and 8(b), which is the same as the result in single factor analysis. However, at 1500 K, the factor of the functional group becomes the most important factor for the thermal conductivity, which has the largest differences of the functional group factor as shown in Fig. 8(c). The single vacancy factor becomes the secondary factor at 1500 K once all the types of defects are added to the MLG. As a result, the influence of the 3 factors on thermal conductivity is ranked as Factor C > Factor B > Factor A at 300 K and 700 K and Factor B > Factor C > Factor A at 1500 K. Figure 9 shows the effect index of each factor, which quantifies the influence of the mean S/N ratio. The effect indexes of the N-doping factor are the smallest at 300 K, 700 K, and 1500 K, which equal 1.51, 1.93, and 1.90, respectively. The effect index of the functional group slightly increases with the temperature, while the effect index of single vacancy sharply decreases with the temperature. At 1500 K, the single vacancy factor becomes the secondary factor with an effect index of 4.39, while the effect index of the functional group is 4.84. As shown in Fig. 8, at 300 K, 700 K, and 1500 K, the total S/N ratios of all the three defects are 13.25, 13.24, and 11.13. The significant decrease in the total S/N ratios at 1500 K can be regarded as the effects of Umklapp scattering. At 1500 K, all the three defects should be affected by the Umklapp scattering. Among them, the decline of vacancy factor importance is the most significant. For N-doping and the -CH_3 groups, the decline of vacancy

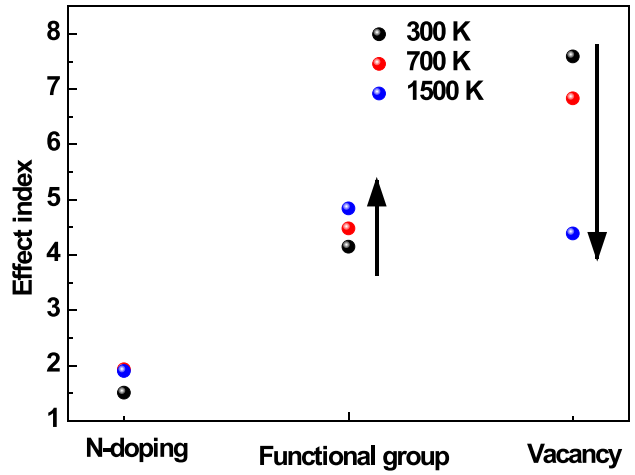

FIG. 9. The effect factor value in terms of the thermal conductivities for the three types of defects at 300 K, 700 K, and 1500 K.

factor importance naturally increases their importance at 700 K and 1500 K.

Based on the sole factor analysis in Sec. III A, the vacancy is the most important factor because the vacancy is the impurity with the highest energy among the three kinds of defects.[10] Besides, the vacancy can excite the extra high-frequency phonon, as shown in Fig. 6(b). Since the Umklapp scattering is weak at 300 K and 700 K,[35,36] the vacancy is still the most important factor in the graphene with the combined defects. Figure 10(a) shows the phonon dispersion relation of MLG with all the types of defects. The phonon dispersion relation is calculated by the SED method, which can be used to study the unexpected weakening of the influence of single defects on the thermal conductivity at 1500 K. The energy band is widened for MLG with the combined defects of 1% N-doping, 2% -CH_3 group, and 1% single vacancy at 300 K. The extra high energy band can also be found in this case. When the single vacancy ratio increases to 4%, the widening becomes more obvious. At 1500 K, the phonon Umklapp scattering is so strong that there is almost no bandgap for the MLG with the combined defects. From the physical point of view, it is hard for the phonon to transport through the graphene sheet smoothly due to the combined effect of Umklapp scattering and defect scattering. In this case, the further increasing amount of single vacancy cannot significantly affect the phonon transport. Figure 10(b) quantitatively shows the phonon lifetimes of the MLG with the combined defects. At 300 K, the increasing amount of single vacancy reduces the lifetimes for all the branches, among which the TA branches decrease from 0.34 ps to 0.19 ps and flexural optical (ZO) branches decrease from 0.36 ps to 0.20 ps. However, the decreasing trend is not significant at 1500 K. The lifetime of the ZO branch is even slightly increased.

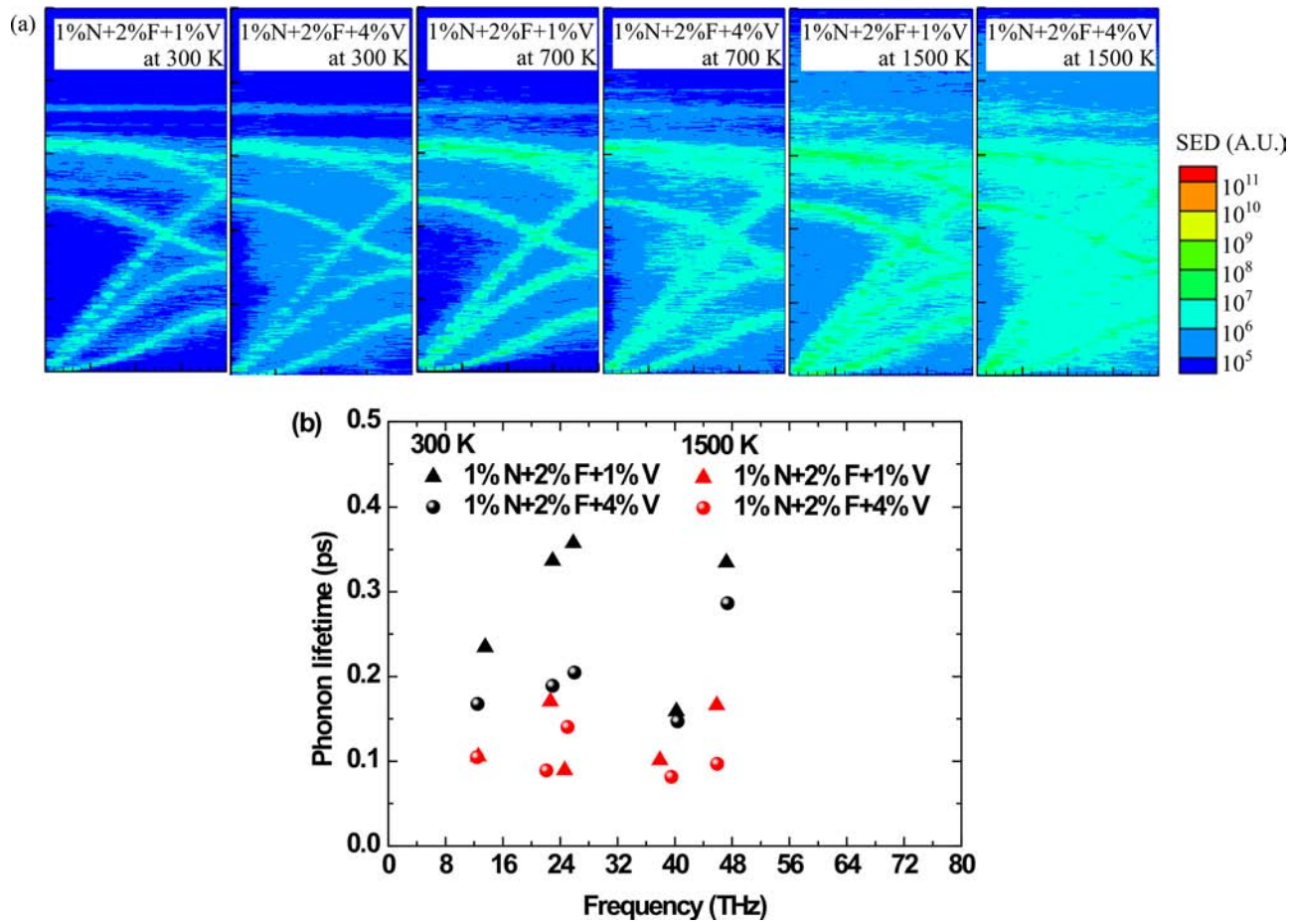

FIG. 10. (a) The phonon dispersion relation of MLG with all the types of defects, where N denotes the N-doping defect, F denotes the functional group defect, and V denotes the vacancy defect. (b) The phonon lifetimes of the MLG at the M point in the first Brillouin zone for MLG with combined defects.

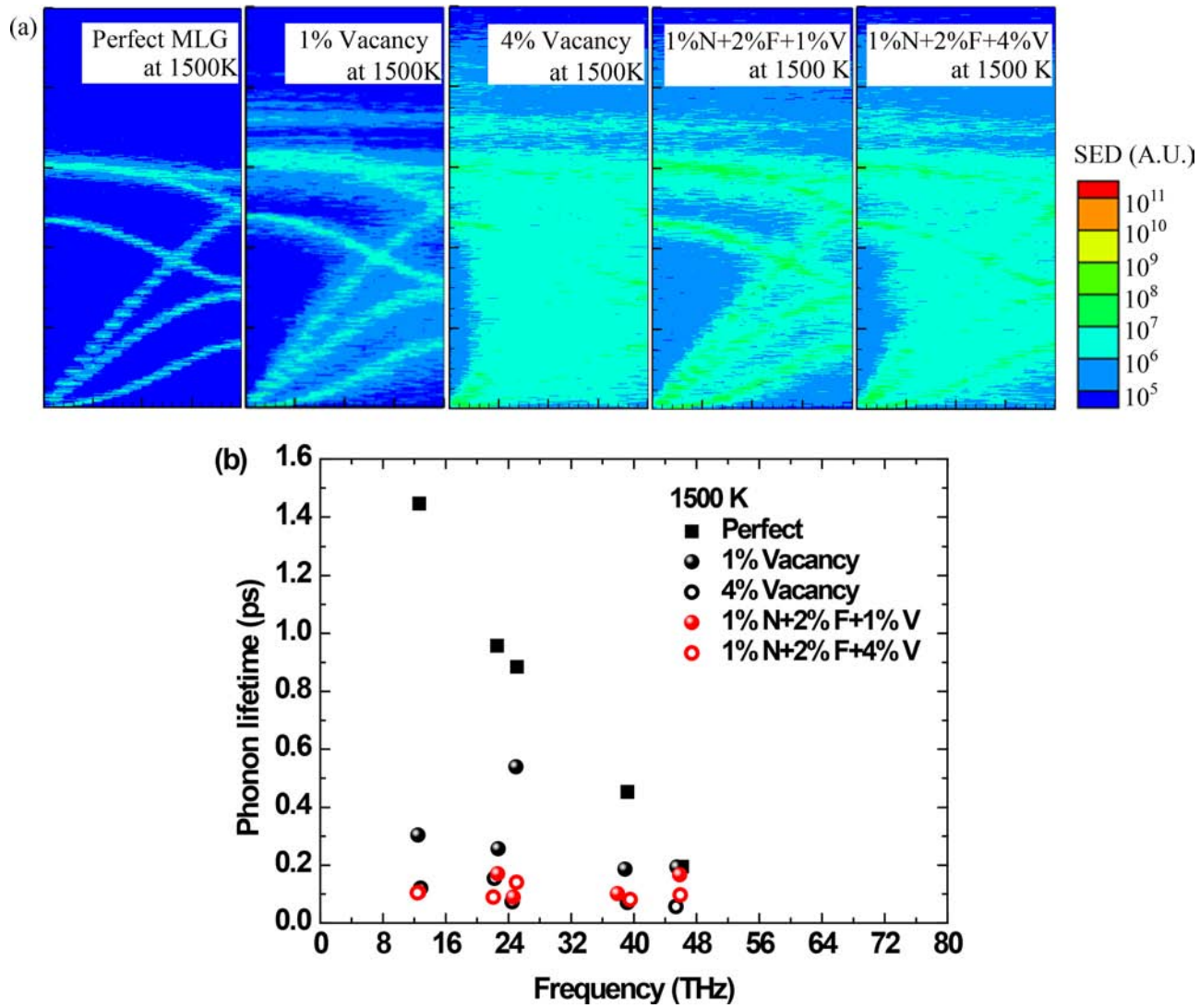

FIG. 11. (a) The phonon dispersion relation of perfect MLG, MLG with 1% and 4% vacancy, and MLG with combined defects of 1% N-doping, 2% -CH_3 group, and 1% vacancy and combined defects of 4% N-doping, 2% -CH_3 group, and 1% vacancy. (b) The phonon lifetimes of the MLG at the M point in the first Brillouin zone for MLG without defects (black squares)/with single vacancies (black circles) and combined defects (red circles).

The perfect thermal property of graphene is related to the clear bandgaps and the high energy density at the energy band. As compared between Figs. 5 and 10(a), the combined effect of all the types of defects on phonon properties occurs in MLG at 300 K, 700 K, and 1500 K. The combined effects at 300 K and 700 K just quantitatively affect the thermal conductivity but do not affect the importance degree of each type of defect. The combined effect at 1500 K decreases the importance of single vacancy. Figure 11(a) shows the phonon dispersion relation of the combined effect at 1500 K. For the case that only single factor is added on the MLG, there are still gaps between the energy bands at 1500 K. Once the amount ratio of the vacancy increases from 1% to 4%, the extra excited phonon can further lead to the decrease in phonon lifetimes, as shown in Fig. 11(b). The reduction of phonon lifetimes from 1% vacancy to 4% vacancy is significant. In addition, for the MLG with combined defects of 1% N-doping, 2% -CH_3, and 1% vacancy, most of the energy gaps are covered due to the impurity scattering and the Umklapp scattering. In this case, the effect of increasing the vacancy amount ratio from 1% to 4% is no longer significant. Figure 11(b) indicates that the phonon lifetimes between the two cases of MLG with combined defects are similar. Therefore, controlling the amount of the single vacancy can facilitate the heat transfer in MLG at 300 K and 700 K, while at 1500 K, the heat transfer can be tuned by controlling either the functional group or single vacancy.

IV. CONCLUSIONS

This work employs the equilibrium molecular dynamics method to study the effects of different types of defects, which includes 1%–4% N-doping, 2%–8% -CH_3 group, or 1%–4% single vacancy, on the thermal conductivity of multi-layer graphene. The sole factor analysis is carried out to compare the effects of different sole types of defects on the thermal conductivity of MLG, and the multi-factor analysis is to reveal the combined effects once all the three types of defects are added on the MLG. The Taguchi orthogonal

algorithm is utilized to analyze the combined effects. The conclusions are obtained as follows:

(1) For the situation that only one type of defect is added into the MLG, at 300 K, 700 K, and 1500 K, the effects of single vacancy on thermal conductivity are the greatest, while the effects of N-doping are the weakest. For the MLG with 4% vacancy defects, the widening phenomena of energy bands in the phonon dispersion relation are obvious. Moreover, unexpected bands can be found in the vacancy cases. Hence, MLG only with N-doping has the largest phonon lifetimes. The vacancy defects can significantly decrease the phonon lifetimes.
(2) Once all the types of defects are added into the MLG, the single vacancy factor plays the most important role on the thermal conductivity at 300 K and 700 K. However, at 1500 K, the -CH_3 group becomes the most important factor that diminishes the thermal conductivity. The combined effect of N-doping, the -CH_3 group, and single vacancy at 300 K and 700 K quantitatively affects the thermal conductivity. At 1500 K, since the Umklapp scattering becomes stronger, almost all the energy gaps in the phonon dispersion relation are covered, which makes the phonon lifetimes very small. Therefore, the effect of vacancy loadings is no longer significant at 1500 K.

ACKNOWLEDGMENTS

This study was partially supported by the National Science Fund for Distinguished Young Scholars of China (No. 51525602), the National Science Fund of China (No. 51606064), the Postdoctoral Science Foundation of China (No. 2016T90071), and the Fundamental Research Funds for the Central Universities (No. 2017ZZD006).

[1]S. Mohammadi, H. Shariatpanahi, F. A. Taromi, and J. Neshati, Mater. Res. Bull. **80**, 7 (2016).
[2]D. M. Curry, H. C. Scott, and C. N. Webster, "Material characteristics of space shuttle reinforced carbon-carbon," in *Proceedings of the 24th National SAMPE Symposium* (San Francisco, CA, 1979), Vol. 24, p. 1524.
[3]W. Torsten and B. Gordon, Mater. Des. **18**, 11 (1997).
[4]F. Hao, D. Fang, and Z. Xu, Appl. Phys. Lett. **99**, 041901 (2011).
[5]Y. Shao, S. Zhang, M. H. Engelhard, G. Li, G. Shao, Y. Wang, J. Liu, I. A. Aksay, and Y. Lin, J. Mater. Chem. **20**, 7491 (2010).
[6]H. C. Schniepp, J. L. Li, M. J. McAllister, H. Sai, M. Herrera-Alonso, D. H. Adamson, R. K. Prud'homme, R. Car, D. A. Saville, and I. A. Aksay, J. Phys. Chem. B **110**, 8535 (2006).
[7]A. Cao and J. Qu, J. Appl. Phys. **111**, 053529 (2012).
[8]W. J. Evans, L. Hu, and P. Keblinski, Appl. Phys. Lett. **96**, 203112 (2010).
[9]E. Pop, V. Varshney, and A. K. Roy, Mater. Res. Bull. **37**, 1273 (2012).
[10]J. Haskins, A. Kınacı, C. Sevik, H. Sevinçli, and G. Cuniberti, ACS Nano **5**, 3779 (2011).
[11]H. Zhang, G. Lee, and K. Cho, Phys. Rev. B **84**, 115460 (2011).
[12]P. Yang, X. Li, Y. Zhao, H. Yang, and S. Wang, Phys. Lett. A **377**, 2141 (2013).
[13]Z. G. Fthenakis, Z. Zhu, and D. Tománek, Phys. Rev. B **89**, 125421 (2014).
[14]T. L. Feng, X. L. Ruan, Z. Q. Ye, and B. Y. Cao, Phys. Rev. B **91**, 224301 (2015).
[15]S. Hu, J. Chen, N. Yang, and B. Li, Carbon **116**, 139 (2017).
[16]J. Hu, S. Schiffli, A. Vallabhaneni, X. L. Ruan, and Y. P. Chen, Appl. Phys. Lett. **97**, 133107 (2010).
[17]H. Zhang, G. Lee, A. F. Fonseca, T. L. Borders, and K. Cho, J. Nanomater. **2010**, 537657 (2010).
[18]B. Mortazavi, A. Rajabpour, S. Ahzi, Y. Rémond, and S. M. V. Allaei, Solid State Commun. **152**, 261 (2012).
[19]S. K. Chien, Y. T. Yang, and C. O. K. Chen, Carbon **50**, 421 (2012).
[20]H. Y. Yang, Y. Q. Tang, J. Gong, Y. Liu, X. L. Wang, Y. F. Zhao, P. Yang, and S. T. Wang, J. Mol. Model. **19**, 4781 (2013).
[21]H. Y. Yang, Y. Q. Tang, Y. Liu, X. Yu, and P. Yang, React. Funct. Polym. **79**, 29 (2014).
[22]M. S. Islam, K. Ushida, S. Tanaka, and A. Hashimoto, Diamond Relat. Mater. **40**, 115 (2013).
[23]H. Malekpour, P. Ramnani, S. Srinivasan, G. Balasubramanian, D. L. Nika, A. Mulchandani, R. K. Lake, and A. A. Balandin, Nanoscale **8**, 14608 (2016).
[24]G. Taguchi, *Introduction to Quality Engineering* (McGraw-Hill, New York, 1990).
[25]R. Kubo, Rep. Prog. Phys. **29**, 255 (1966).
[26]S. Plimpton, J. Comput. Phys. **117**, 1 (1995).
[27]L. Lindsay and D. A. Broido, Phys. Rev. B **81**, 205441 (2010).
[28]A. Kınacı, J. B. Haskins, C. Sevik, and T. Cağın, Phys. Rev. B **86**, 115410 (2012).
[29]S. J. Stuart, A. B. Tutein, and J. A. Harrison, J. Chem. Phys. **112**, 6472 (2000).
[30]J. Li, L. Porter, and S. Yip, J. Nucl. Mater. **255**, 139 (1998).
[31]J. R. Lukes and H. L. Zhong, J. Heat Transfer-Trans. ASME **129**, 705 (2007).
[32]J. A. Thomas, J. E. Turney, R. M. Iutzi, C. H. Amon, and A. J. H. McGaughey, Phys. Rev. B **81**, 081411 (2010).
[33]W. H. Chen, S. R. Huang, and Y. L. Lin, Appl. Energy **158**, 44 (2015).
[34]D. Wei, Y. Liu, Y. Wang, H. Zhang, L. Huang, and G. Yu, Nano Lett. **9**, 1752 (2009).
[35]C. Si, X. D. Wang, Z. Fan, Z. H. Feng, and B. Y. Cao, Int. J. Heat Mass Transfer **107**, 450 (2017).
[36]A. Cao, J. Appl. Phys. **111**, 083528 (2012).
[37]G. C. Loh, E. H. T. Teo, and B. K. Tay, Diamond Relat. Mater. **23**, 88 (2012).